

# Thermal Properties of Plasma-Sprayed $(\text{La}_{0.4}\text{Sm}_{0.5}\text{Yb}_{0.1})_2\text{Zr}_2\text{O}_7$ Coatings on NiCrCoAlY Bond Coats

Liu Ling<sup>1,2</sup>, Wang Fuchi<sup>1,2</sup>, Ma Zhuang<sup>1,2</sup>, Sun Yingchao<sup>1,2</sup>

<sup>1</sup> Beijing Institute of Technology, Beijing 100081, China; <sup>2</sup> National Key Laboratory of Science and Technology on Materials under Shock and Impact, Beijing 100081, China

**Abstract:**  $(\text{La}_{0.4}\text{Sm}_{0.5}\text{Yb}_{0.1})_2\text{Zr}_2\text{O}_7$  (LSYZO) coating was prepared by atmospheric plasma spray.  $\text{Sm}_2\text{Zr}_2\text{O}_7$  (SZO) coating was also prepared in the same conditions as a contrast. Microstructures and phases of LSYZO coatings were investigated by scanning electrical microscopy (SEM) and X-ray diffraction (XRD), respectively. The thermal conductivities of the two coatings were measured. The results show that the phase composition of LSYZO coating has no change after plasma spraying. The adhesion strength of LSYZO coating is 22 MPa, which is comparable with that of SZO coating. And LSYZO coating has lifetime of about 40 cycles. The thermal conductivity of LSYZO coating is lower than that of SZO coating, which mainly depends on the complex structure of LSYZO ceramic.

**Key words:** rare-earth zirconates; thermal properties; thermal barrier coatings

In recent years, thermal barrier coatings (TBCs) have been widely used in advanced aircraft and industrial gas-turbine engines, in order to enhance the reliability and durability of hot-section metal components as well as the efficiency of engines. Use of TBCs can result in significant temperature decrease between hot gas and surface of these components. In the next generation of advanced engines, further increase in thrust-to-weight ratio will be required, even higher gas temperatures<sup>[1,2]</sup>. To meet this requirement, exploring new advanced TBCs with higher reliability and lower thermal conductivity to substitute conventional YSZ coatings is very essential. Recent development efforts have focused towards pyrochlore-structured oxides of general composition, such as  $\text{La}_2\text{Zr}_2\text{O}_7$ ,  $\text{Sm}_2\text{Zr}_2\text{O}_7$  (SZO), and  $\text{Dy}_2\text{Zr}_2\text{O}_7$ . The results show that these materials are promising as top ceramic materials for future thermal barrier coatings, because of their high melting point, low thermal conductivity and excellent thermal stability<sup>[3,4]</sup>.

At present, there is an increasing demand to develop pyrochlore oxide compounds with better properties. The recent researches indicate that substituted cation at site A or

B in the simple pyrochlore oxides can improve both the thermal conductivity and the thermal expansion coefficient<sup>[5,6]</sup>. A series of new rare-earth zirconates have been reported<sup>[7,8]</sup>. However, most of the studies on complex rare earth zirconates focus on the thermophysical properties of the ceramics only. Few reports on the properties of their coatings have been published. In our former work,  $(\text{La}_{0.4}\text{Sm}_{0.5}\text{Yb}_{0.1})_2\text{Zr}_2\text{O}_7$  (LSYZO) ceramic was designed and successfully prepared, while the thermophysical properties of this material were proved to be excellent<sup>[9]</sup>. In this paper, LSYZO coating was prepared by atmospheric plasma spray. The thermal conductivity, adhesion strength and thermal shock resistance of the coating were investigated. As a comparison, SZO coating was prepared under the same conditions, and the relative properties were studied.

## 1 Experiment

LSYZO precursor was synthesized by a coprecipitation-calcination method<sup>[9]</sup>, and then calcined at 1250 °C for 5 h to obtain pyrochlore structure. In order to improve the fluidity, the as-synthesized powder was ground and granu-

lated by ball-milling with the 10 wt% PVA as binder. Finally, spherical agglomerated particles were obtained, and the particle size in the range of 20~80  $\mu\text{m}$  was chosen for plasma spraying. Commercial NiCoCrAlY powders with chemical composition (wt%) of Ni-21Co-17Cr-12Al-1Y were chosen for spraying the bond coatings of TBCs.

NiCrCoAlY bond coats were firstly deposited onto disk shaped mild steel substrate. Then the APS-5500 atmosphere plasma spraying system equipped with a SG-100 plasma gun (Praxair Surface Technologies, USA) was applied to deposit LSYZO coatings. Meanwhile, SZO coating was also produced in the same conditions as a contrast. The plasma spraying parameters were listed in Table 1. To obtain free-standing samples used in this work, coating of about 2 mm thickness was deposited onto a graphite substrate with Ar and He as plasma primary and auxiliary gases and then it was removed from the substrate by a mechanical method.

Crystal-phase identification of the synthesized powders after calcination and the coatings was determined by X-ray diffractometry (XRD, RIGAKU D/Max-rB, Rigaku International Corp, Sendagaya, Shibuya-Ku, Tokyo, Japan) at a scan rate of 4  $^\circ/\text{min}$ . The surface and cross-sectional microstructure of SZO and LSYZO coatings were examined using scanning electron microscopy (SEM, Philips S-4800, Hitachi Ltd., Yoshida-Cho, Totsuka-Ku, Yokohama, Japan). The thermal diffusivity ( $\lambda$ ) for the two coatings was measured, using the laser-flash method (Model FLASHLINE 5000, Anter Corp., Pittsburg, USA), as a function of specimen temperature in an argon atmosphere. The specimens for thermal diffusivity measurement with dimensions of  $\Phi$  12.7 mm $\times$ 1.0 mm were machined. As experimental heat capacity ( $C_p$ ) data are not available, heat capacity values for the present materials were obtained employing the Neu-

mann-Kopp rule<sup>[10]</sup>. Based on the above rule, the molar heat capacities of the samples were calculated as a weighted sum of heat capacities of the constituent binary oxides (namely,  $\text{La}_2\text{O}_3$ ,  $\text{Sm}_2\text{O}_3$ ,  $\text{Yb}_2\text{O}_3$  and  $\text{ZrO}_2$ ). Heat capacity data for the constituent binary oxides were taken from thermodynamic data handbook of inorganic compounds<sup>[11]</sup>. Measurement of the density of the samples was carried out by the liquid immersion technique using distilled water as the immersion liquid. The thermal conductivity  $k$  was calculated as shown in Ref. [12]. The bonding strength test was performed by electronic universal tensile machine (Model WDW-E100, Anduo Trade Co. Ltd, Nanjing, China). The coatings were bonded to metal stainless steel cylinder using a cold-cured adhesive glue to investigate the mechanical adhesion strength. The thermal shock test was carried out by a heating and water quenching method. Each cycle consisted of 20 min holding specimens in a furnace at 1100  $^\circ\text{C}$ , followed by direct quenching into water. The lifetime of the coatings was defined by the number of cycles at which 20% of total coatings surface area was peeled or delaminated. Each kind of coating took three samples to estimate lifetime

## 2 Results and Discussion

XRD patterns of LSYZO powders after calcination and the coatings as-sprayed are given in Fig.1. Fig.1 indicates that the X-ray diffractograms of the powders and coatings are both coincident with the standard spectrum of samarium zirconates with single pyrochlore structure. It shows that phase of the LSYZO coatings has no difference from that of the corresponding powders. It indicates that there is no phase change in the plasma spray process, and LSYZO material shows good phase stability during spray deposition.

**Table 1 Parameters of plasma spraying**

Coatings	Current/ A	Primary gas Ar (scfh*)	Secondary gas He (scfh*)	Carrier gas Ar (scfh*)	Powder feed rate/r min <sup>-1</sup>	Distance/ mm
Bond coating	700	20	10	10	2.5	75
Top coating	900	60	50	10	4.0	65

\* scfh=standard cubic feet perhour

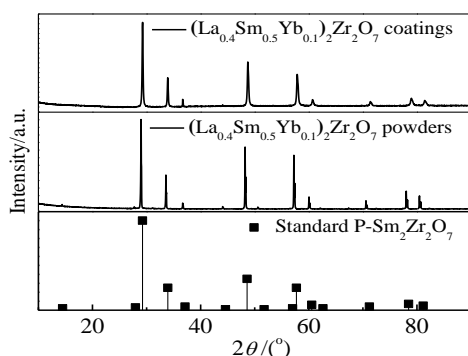


Fig.1 XRD patterns of LSYZO powders and coatings

The surface and cross-sectional morphology of LSYZO coating are shown in Fig.2. As seen in Fig.2a, some unmelted particles on the surface of micro-structured TBCs are observed. Because of the shrinkage of melted particles after spraying to room temperature, some micro-cracks also exist in both coatings. The cross-sectional morphology of the coating in Fig.2b indicates that LSYZO coating demonstrates a dense state. A lamellar structure made of mechanically interlocking molten splats and low micro-scaled porosities are the characteristics of LSYZO TBCs. The value for porosities of SZO and LSYZO coatings is 7.3% and 6.8%, respectively.

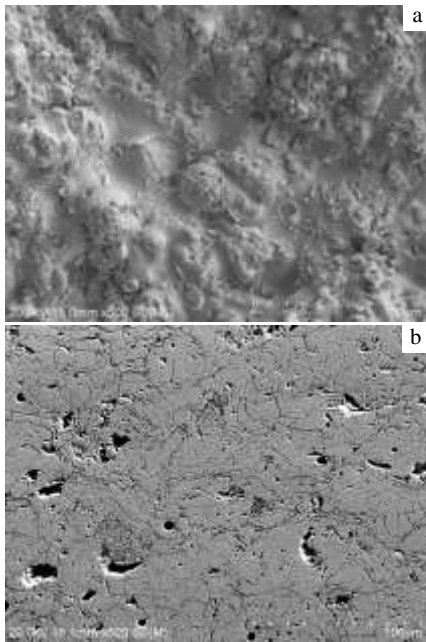


Fig.2 Surface (a) and cross-sectional (b) morphologies of LSYZO coatings

Heat capacity value of LSYZO for various temperatures is calculated. According to the calculated results, in the whole temperature range, the heat capacity of LSYZO can be fitted as Eq. (1).

$$C_p = 0.42775 + 9 \times 10^{-5}T - 120.29404T^{-2} \quad (1)$$

The thermal conductivity of SZO and LSYZO coatings is shown in Fig.3. It can be seen that with the considerable porosity, the thermal conductivity of LSYZO coating at  $0.57 \sim 0.75$  W/m K is obviously lower than that of SZO coating ( $0.7 \sim 0.9$  W/m K). Therefore, LSYZO coating shows better heat insulation than SZO coating, which mainly depends on the complex structure of LSYZO ceramic [9]. Compared to that of YSZ coating with 15.7% porosity (about  $0.93$  W/m K at  $900$  °C) [6], the thermal conductivity of LSYZO coating is significantly lower though its porosity is low.

The result of adhesion strength shows that an average value of  $22$  MPa is achieved in the LSYZO coating, which is comparable with that of SZO coating about  $20$  MPa. The tensile fractured microstructures of both coatings are similar. The fractured images of LSYZO coating are displayed as an example. From the fractured macrostructure of LSYZO coating in Fig.4a, the fracture occurs mainly at the interface between the ceramic layer and bond layer. Fig.4b demonstrates that LSYZO coating consists of splats aligned predominantly parallel. One layer bonds closely with another. The columnar grain structure is obvious. There are also

some unmelted particles and equiaxed grains at individual regions. The relatively loose structure may weaken lamellar bonding.

SZO coating exhibits a lifetime of 60 cycles, while spallation failure of the LSYZO coating occurs after around 40 cycles. Fig.5 shows a photograph of SZO and LSYZO coatings after thermal shock. Spallation failure is visible along both samples rim, which is usually a failure mechanism for TBC due to the singularity of thermal stresses at the rim. Fig.6 shows the cross-sectional microstructures of SZO and LSYZO coatings after thermal shock. It can be seen that, after thermal shock, there are many short horizontal cracks, large holes and loose regions in the

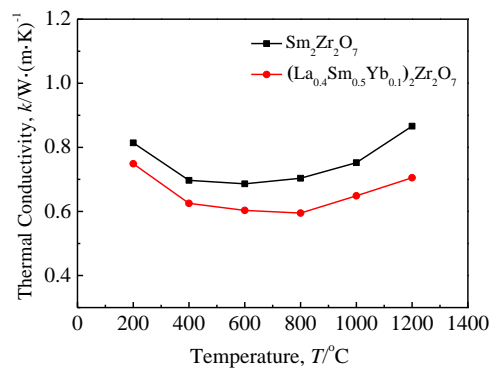


Fig.3 Thermal conductivity versus temperature for SZO and LSYZO coatings

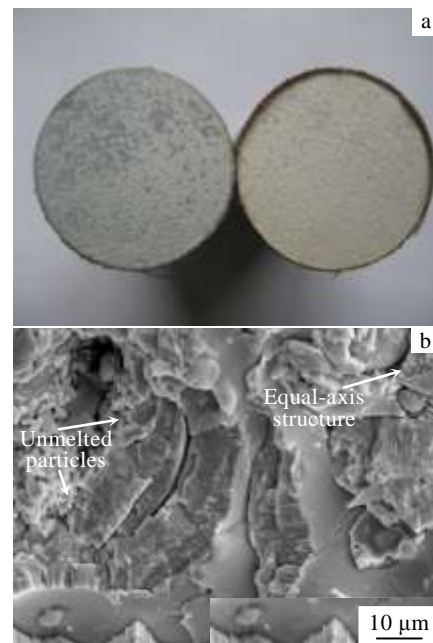


Fig.4 Low (a) and high amplification (b) fractured morphology of LSYZO coatings

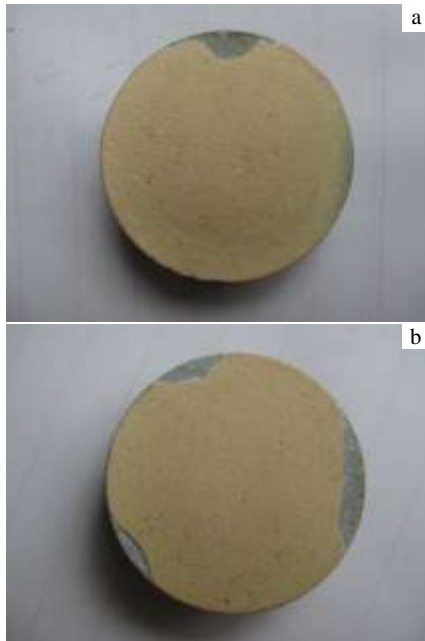


Fig.5 Macrostructures of the two coatings after thermal shocking: (a) SZO and (b) LSYZO

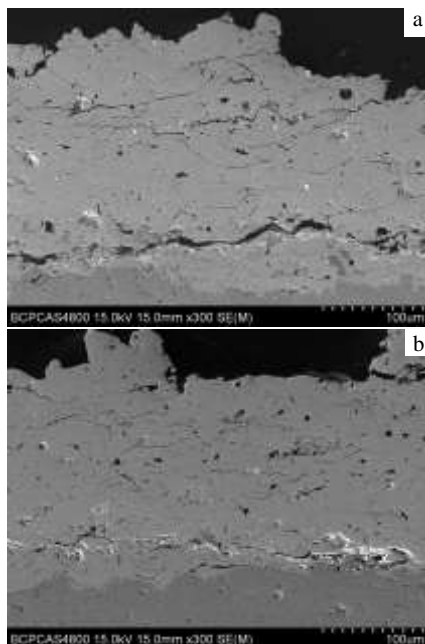


Fig.6 Cross-section microstructure of the two coatings after thermal shocking: (a) SZO and (b) LSYZO

top coat. Penetrating cracks are the main type of cracks near the interface between the top coat and bond coat. Cracks in LSYZO coating are more than that in SZO coating. The emergence of horizontal crack is due to axial stress generated by the different thermal expansion coefficients be-

tween top coat and the bond coat<sup>[13]</sup>. According to the previous test result of thermal expansion for SZO and LSYZO, the intrinsic thermal expansion coefficient of LSYZO material ( $\sim 10.3 \times 10^{-6}$  at 1300 °C) is lower than that of SZO ( $\sim 10.8 \times 10^{-6}$  at 1300 °C)<sup>[9]</sup>. At high temperature, the difference of thermal expansion between LSYZO top coat and bond coat increases, which generates large axial thermal stress at the interface. In the thermal shock process, the pores are expanded and compressed circularly by axial stress, and then micro-cracks form<sup>[14]</sup>. Large axial stress in LSYZO coating makes the internal micro-cracks grow faster, which leads to final failure. That is why the thermal cycling lifetime of LSYZO coating is shorter than that of SZO coating.

### 3 Conclusions

1) Pure  $(La_{0.4}Sm_{0.5}Yb_{0.1})_2Zr_2O_7$  powder and coating are prepared by chemical coprecipitation and atmospheric plasma spraying process. The phase composition of LSYZO coating has no change before and after thermal spraying, which suggests that this material shows good phase stability during spray deposition.

2) The thermal conductivity of LSYZO coating is lower than that of SZO and YSZ coatings, which mainly depends on the complex structure of LSYZO ceramic. The adhesion strength of LSYZO coating is 22 MPa, which is comparable with that of SZO coating.

3) The thermal cycling lifetime of LSYZO coating is about 40 cycles, which is shorter than that of SZO coating. The worse performance of LSYZO coating is mainly due to its poor intrinsic thermal expansion coefficient.

### References

- 1 Saint R B. *Air and Space Europe*[J], 2001, 3(3-4): 174
- 2 Pan W, Wan C L, Xu Q. *Thermochemica Acta*[J], 2007, 455(1-2): 16
- 3 Wu J, Wei X Z, Padture N P. *Journal of the American Ceramic Society*[J], 2002, 85(12): 3031
- 4 Clarke D R, Levi C G. *Annual Review of Materials Research*[J], 2003, 33(1): 383
- 5 Winter M R, Clarke D R. *Acta Materialia*[J], 2006, 54(19): 5051
- 6 Bansal N P, Zhu D M. *Materials Science and Engineering A*[J], 2007, 459(1-2): 192
- 7 Liu L, Xu Q, Wang F C et al. *Journal of the American Ceramic Society*[J], 2008, 91(7): 2398
- 8 Liu L, Wang F C, Ma Z et al. *Journal of the American Ceramic Society*[J], 2011, 94(3): 675
- 9 Liu L, Wang F C, Xu Q et al. *Key Engineering Materials*[J], 2012, 512: 469
- 10 Leitner J, Chuchvalec P, Sedmidubsky D. *Thermochemica Acta*[J], 2003, 395(1): 27
- 11 Liang Y J, Che Y C eds. *Thermodynamic Data Handbook of Inorganic Compounds*[M]. Shenyang: Northeast University

Press, 1993: 423 (in Chinese)

641

12 Xu Q, Pan W, Wang J D. *Materials Letters*[J], 2005, 59(22): 2804

14 Guo H B, Vaben R, Stover D. *Surface and Coatings Technology*[J], 2005, 192: 48

13 Ahmet P, Ozkan S, Erdal C. *Materials Design*[J], 2003, 23(7):

## NiCrCoAlY 粘结层表面等离子喷涂(La<sub>0.4</sub>Sm<sub>0.5</sub>Yb<sub>0.1</sub>)<sub>2</sub>Zr<sub>2</sub>O<sub>7</sub> 涂层的热性能研究

刘 玲<sup>1,2</sup>, 王富耻<sup>1,2</sup>, 马 壮<sup>1,2</sup>, 孙英超<sup>1,2</sup>

(1. 北京理工大学, 北京 100081)

(2. 冲击环境国家重点实验室, 北京 100081)

**摘 要:** 采用大气等离子喷涂制备了(La<sub>0.4</sub>Sm<sub>0.5</sub>Yb<sub>0.1</sub>)<sub>2</sub>Zr<sub>2</sub>O<sub>7</sub> (LSYZO)涂层, 并在相同的条件下制备了Sm<sub>2</sub>Zr<sub>2</sub>O<sub>7</sub>涂层作为对比。分别用扫描电子显微镜 (SEM) 和X射线衍射仪 (XRD) 分析 LSYZO涂层的微观形貌和相结构, 并对2种涂层的热导率进行测定。结果表明, 等离子喷涂后LSYZO涂层的相结构未发生变化。LSYZO涂层的结合强度为22 MPa, 与SZO涂层相当。LSYZO涂层热震 40次后发生失效, 其热导率明显低于SZO涂层, 这主要与LSYZO陶瓷自身的复杂结构有关。

**关键词:** 稀土锆酸盐; 热性能; 热障涂层

---

作者简介: 刘 玲, 女, 1982 年生, 博士, 副教授, 北京理工大学材料学院, 北京 100081, 电话: 010-68911144, E-mail: richard@bit.edu.cn